

Yttrium-Stabilized Zirconia Particles Prepared Using Electro-dialysis of (Zr,Y)OCl₂ Aqueous Solution

Myung Chul Chang[†]

Department of Materials Science and Engineering, Kunsan National University, Gunsan 573-701, Korea

(Received August 19, 2013; Revised June 2, 2014; Accepted September 8, 2014)

ABSTRACT

Hydrous zirconia particles were prepared from ZrOCl₂ aqueous solution using an electro-dialysis [ED] process. For the preparation of (Zr,Y)(OH)₄ precipitates, 3 mol% YCl₃ was added into ZrOCl₂ aqueous solution. During the hydrolysis of 0.5 mol/L (Zr,Y)OCl₂ solution at 90°C a slurry solution was obtained. The ED process was used for the removal of chlorine from the slurry solution. Two kinds of slurry solution were sampled at the beginning and end of the ED process. The morphology of hydrous zirconia particles in the solution was observed using an inverted optical microscope and an FE-SEM. The hydrous zirconia particles were nano-crystalline, and easily coagulated with drying. Yttrium stabilized zirconia [YSZ] powder could be obtained by the calcination of (Zr,Y)(OH)₄ precipitates prepared from a (Zr,Y)OCl₂ solution by the ED process. The coagulated dry powders were shaped and sintered at 1500°C for 2 h. The sintered body showed a dense microstructure with uniform grain morphology.

Key words : Hydrous zirconia, Zirconium oxychloride, Electrodialysis, Nano-particles, Anion membrane

1. Introduction

Stabilized tetragonal zirconia polycrystal [TZP] ceramics are extremely tough and mechanically strong, and the hydrolysis of ZrOCl₂ solution¹⁻⁶⁾ is a typical process for preparation of TZP powders. An aqueous solution of ZrOCl₂ is mixed with stabilizing components of Y, Ce, Ca, and/or Mg salt compounds,^{7,8)} and the mixed solution is hydrolyzed to make hydrous zirconia particles. The prepared nano-particles are then dried and calcined for final processes such as forming and sintering. In particular, the quality of TZP granule powders is greatly influenced by the process used to form the hydrous zirconia. According to Clearfield,^{1,2)} the aqueous ZrOCl₂ solution was hydrolyzed at pH 1–2.5 by the addition of aqueous NH₄OH (Fig. 1) and monoclinic, nano-crystalline particles of hydrous zirconia were formed. According to Hevesy,⁹⁾ hydrous zirconia particles were prepared in ZrOCl₂ at a concentration of 0.055 mol/L, and their morphology, as observed by TEM, was nano-crystalline with a diameter of 50 nm. From primary particles of hydrous zirconia, a crystalline structure was formed as a result of strong aggregation of monoclinic crystal nuclei (≤ 10 nm diameter).¹⁰⁾

In this research, the aqueous solution of (Zr,Y)OCl₂ was hydrolyzed, and then an electro-dialysis [ED] process^{11,12)} was applied to the solution. The use of the ED process for the (Zr,Y)OCl₂ solution was very effective for preparing

hydrous zirconia particles without chlorine residue. The particle morphology of the prepared hydrous zirconia was determined using an optical microscope and an FE-SEM. The hydrous zirconia particles thus obtained were dried and shaped for investigation of their sintering behavior. The sin-

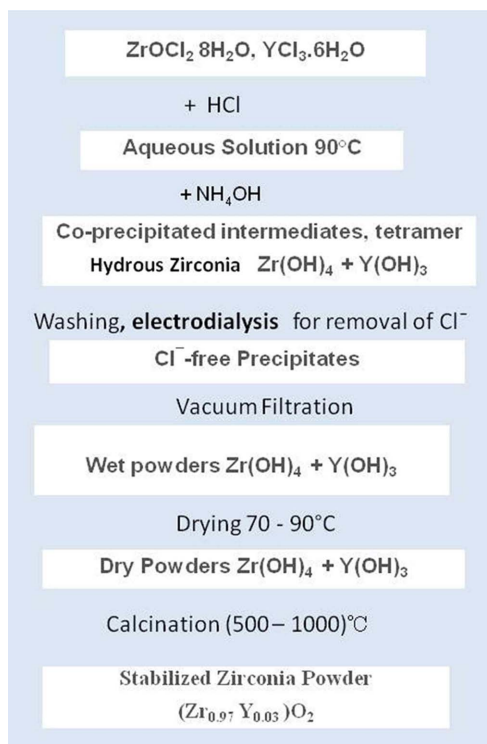


Fig. 1. Precipitation process of yttrium stabilized zirconia powders.

[†]Corresponding author : Myung Chul Chang

E-mail : mcchang@kunsan.ac.kr

Tel : +82-63-469-4735 Fax : +82-63-462-6982

tered samples were very dense and their grain size was uniform. In order to control the hydrolysis process, the acid dissociation of the ZrOCl₂ solution³⁻⁶⁾ was investigated.

2. Experimental Procedure

2.1. Preparation of (Zr,Y)OCl₂ solution and hydrolysis

In the flow diagram of the co-precipitation process in Fig. 1, ZrOCl₂·8H₂O (99.0% purity, Sigma Aldrich) was dissolved in deionized [DI] H₂O. From Fig. 2,^{9,10)} the concentration of ZrOCl₂ was 0.5 mol/L in DI water, as a hydrolysis solution, and the corresponding [HCl] was estimated to be 2.5 mol/L. From the temperature dependence in Fig. 2(a), the required amount of [ZrOCl₂] in 100 cc H₂O solution was 28 g at 90°C, as shown in the closed rectangles. Furthermore, YCl₃·6H₂O (99.0% purity, Sigma Aldrich) was added in order to prepare a (Zr_{0.97}Y_{0.03})OCl₂ solution.

The starting precursors of ZrOCl₂·8H₂O and YCl₃·6H₂O were dissolved in DI H₂O in a beaker while stirring, and then the mixed solution was heated to 90°C while stirring. As shown in Fig. 2(b) and (c) the proper amount [0.0027 - 0.0082 mol/L] of HCl was added to the mixed solution to adjust the pH to 1.0.¹⁵⁻¹⁷⁾ Aqueous ammonia solution was

prepared by mixing 40 mL NH₄OH and 160 mL DI H₂O. This was then added to the mixed solution for a co-precipitation reaction at pH 1.2. The precipitation process at 90°C was achieved by dripping aqueous ammonia solution into the (Zr,Y)OCl₂ aqueous solution while stirring. It took one hour for the preparation of 18 g of Zr(OH)₄ slurries (Fig. 2(a)) and the slurry particles were barely visible in the solution. Next, the slurry solution was transferred into the ED membrane reactor (Fig. 3) to remove the chlorine through the ED process.

Reference samples were prepared at pH 2.0 - 4.0 (Fig. 2(c)) using the precipitation process. We used 0.5 M aqueous solution of (Zr,Y)OCl₂ and the alkali solution was a mixture of 40 mL NH₄OH and 190 mL DI H₂O. Their pH values were estimated to be pH 1.44 and pH 10.75 at room temperature, respectively. Both solutions were dripped into a beaker being stirred by a Masterflex pump and pH controller.^{13,14)} The droplets of both solutions were precipitated at pH 4.0 and it took about 70 min for the full consumption of solution of (Zr,Y)OCl₂. The volume was considerably larger than that of the precipitates prepared at pH 1.2. The precipitates were washed in a vacuum aspirator using DI H₂O and a glass filter. The sample weights were found to be 6.7608 g and 4.5382 g after drying at 100°C, and calcination at

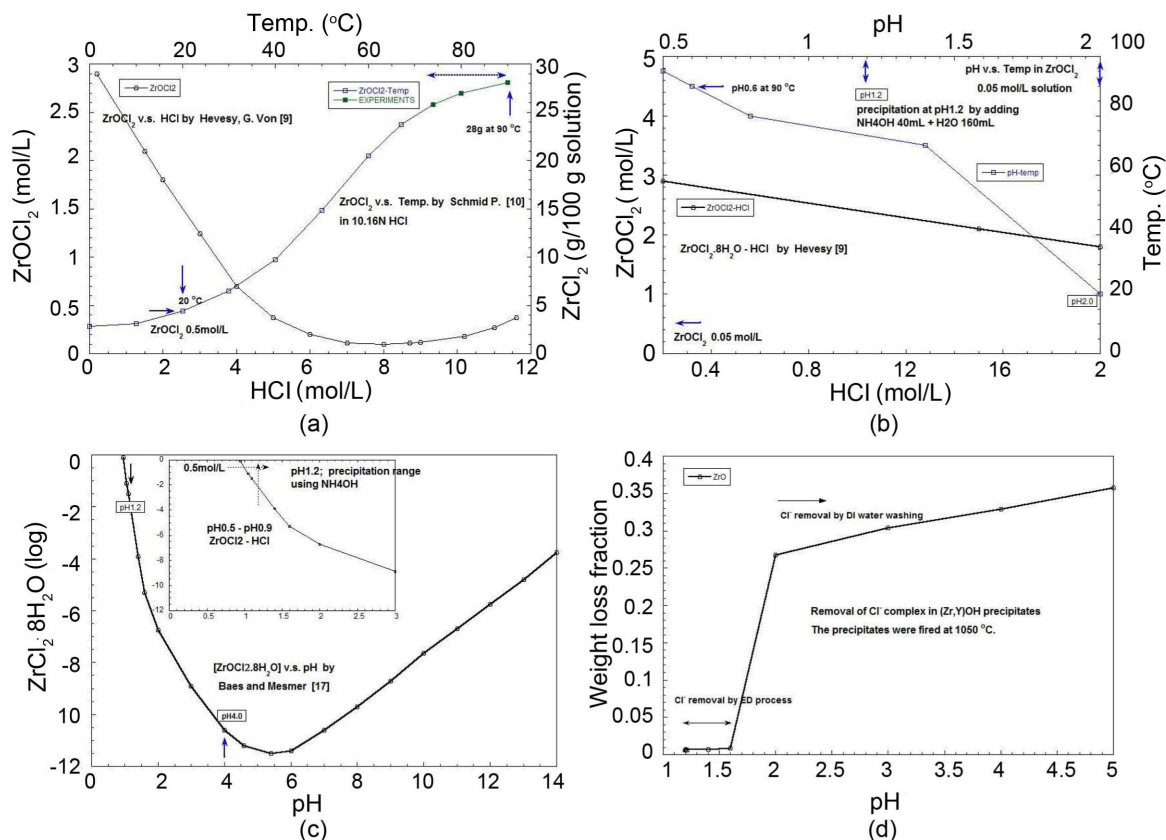


Fig. 2. (a) The solubility of zirconyl chloride octahydrate at various concentration of hydrochloric acid and (b) Temperature effect on the solubility of zirconyl chloride in hydrochloric acid. Left: The solubility of zirconyl chloride octahydrate at various concentration of hydrochloric acid and Right: The pH change with the variation of temperature. (c) The solubility diagram between concentration of zirconyl chloride octahydrate and pH values and (d) The weight change of dry precipitates, which were prepared with the pH change, after calcination at 1050°C.

1050°C, respectively. The weight loss after calcination was 32.87%. The sample prepared at pH 2.0 showed a weight loss of 28.157%. The sample weights were found to be 5.0239 g and 3.6093 g after drying at 100°C, and calcination at 1050°C, respectively. As plotted in Fig. 2(d) the weight change of the reference samples was much greater than that of the precipitates obtained at pH 1.2 by the ED process. The precipitates prepared at pH 1.2 were nano-crystalline and the ED process was very effective at chlorine removal.

2.2. Removal of Cl^- from the hydrous zirconia solution in the ED reactor

A mixed solution of hydrolyzed (Zr,Y)-OH-Cl was transferred into a reaction chamber with a cathode (Fig. 3). An anion membrane [AMV, Selemion, Asahi Chemical] in the ED reactor was used for Cl^- exchange. Under DC power the Cl^- ions in the cathode reactor moved into the anode chamber via ion exchange through the AMV membrane. The reactor was made using a transparent HDPE plastic container to which the AMV membrane was bonded to the inner surface using additives [3M DP-8005]. Pt and Ti electrode sieves were used as the anode and cathode.

During the ED process, increased DC power resulted in decrease of $[\text{Cl}^-]$ in the cathode reactor, and increase of $[\text{Cl}^-]$ in the anode reactor. In the initial stage of the ED process, higher voltage (between 30 and 50 V) was applied and then the solution in the reactor began to heat. Both chambers of cathode and anode were gradually heated during the ED reaction because of the exothermic reaction of Cl^- with H_2O . During the de-chlorination process, the reaction temperature increased and temperatures above 40°C can result in the rapid degradation of ion change membrane. In order to protect the ion exchanging ability of the membrane, the aqueous solution of the anode reactor was periodically flushed with fresh DI water. During the entire ED reaction, the temperature of reaction chambers was kept under 40°C to preserve the membrane quality. The flow of water at the inlet and outlet was operated at pH values above 3.0 in the cathode chambers, and above 5.0 in the anode chamber. The

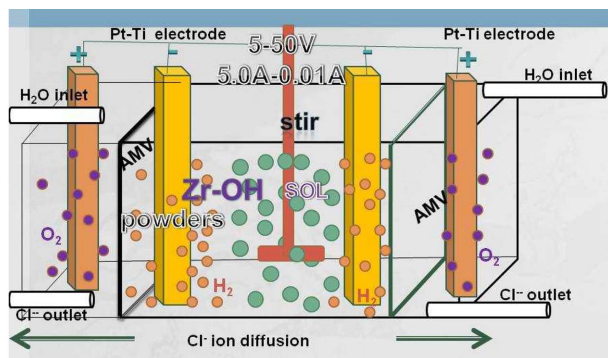


Fig. 3. Schematic design of electrodiagnosis reactor system using anionic membrane [AMV]. The AMV membrane from Asahi Chemistry Co. Pt-Ti electrodes were used for cathode and anode, respectively.

DC power was operated in the range of 20 - 50 V and 1.0 - 5.0 A using an automatic I-V controller [power supply GP4505-DU, Gold Star]. After 2 h of the ED reaction, gel-like particles could be observed in the transparent solution. The amount of gel-like particles increased with increasing de-chlorination time. Eventually, the slurry solution got highly viscous and the color got yellowish. The maximum current value decreased with increasing ED-reaction time and solid white particles were visible an hour after the appearance of the above-mentioned gel-like particles. As the number of solid white particles increased, the slurry solution got less viscous. After one day, the de-chlorination current dropped under 0.03 A. This was considered an indication of the completion of the ED reaction. After termination of the ED reaction, the hydrous zirconia precipitates in the main reactor were transferred into a beaker and stirred for several hours. The hydrous zirconia precipitates were washed in a vacuum filter using DI H_2O , and finally in a solution of ethyl alcohol to control particle coagulation.

The wet slurry was dried at 70°C and put into alumina crucibles for calcination at 675, 750, or 800°C for 2 h. Stabilized zirconia $\text{Zr}_{1-x}\text{Y}_x\text{O}_2$ ($x = 0.03$ mole%) powder was obtained. The YSZ powders were mixed with a small amount of PVA binder and pressed uniaxially using a stainless-steel mold. The shaped sample was pre-sintered at 1100°C for 2 h and the samples obtained were finally sintered at 1500°C for 2 h.

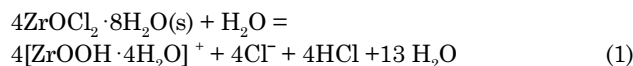
2.3. Characterization

During the de-chlorination process, a small amount of the slurry being formed was extracted from the main reactor and the slurry morphology observed using an optical microscope [OM, Olympus IX51] and FE-SEM [Hitachi, S-4800]. During the OM observation the slurry solution gradually dried and its morphology changed. One of the recorded virtual OM images is presented in Fig. 4(a) and (b). XRD [Bruker, M18XCE] was used to characterize the dried powders after termination of the ED process. The microstructure of the sintered body was determined using the FE-SEM.

3. Results and Discussion

3.1. Preparation of hydrous zirconia

It is known^{1,2,15-18}) that in an aqueous solution of $\text{ZrOCl}_2 \cdot 8\text{H}_2\text{O}$, the predominant zirconium species include the $[\text{Zr}_4(\text{OH})_8]^{8+}$ ion and zirconium polymers, in which water molecules are grouped, and which decompose into units of ZrOOH^+ . This cationic hydrolysis product is characteristic of zirconium complexes^{2,19}) in a chlorine environment. The hydrolysis process can be written as:



The presence of excess hydronium $[\text{H}_3\text{O}^+]$ ions forces the

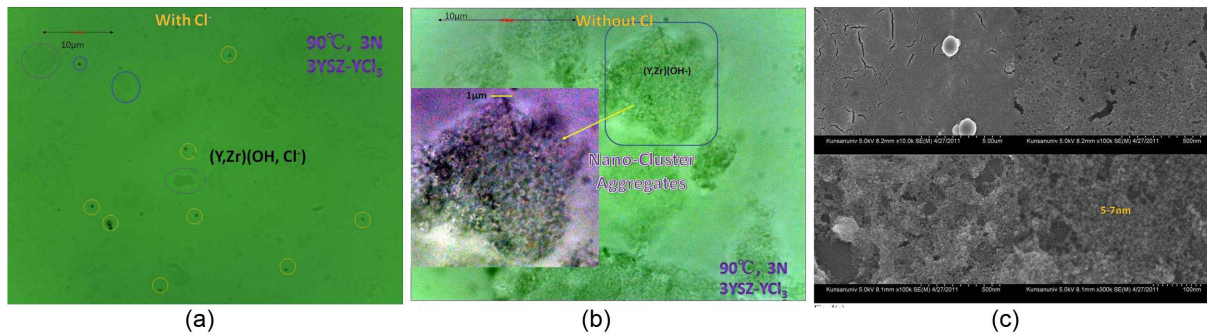
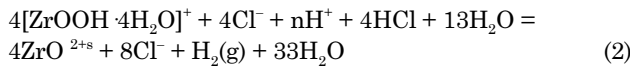
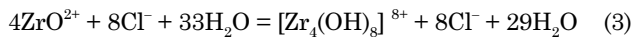


Fig. 4. Optical micrographs for the slurry paste dropped on the slide in the initial stage of ED process (a) the first image of slurry morphology after the drop on slide, (b) the image of agglomerated particles after several minutes of dropping. The drying induced the agglomeration, and (c) SEM micrographs for the dry samples of the slurry paste.

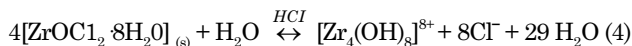
hydrolysis product on to the next state.



Further hydrolysis of this metastable hydrous zirconia ion results in:



The overall hydrolysis of the solid zirconyl chloride can be summarized as:



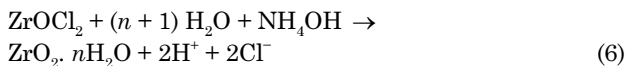
Equations (1) - (3) are combined in Eq. (4) by the addition of HCl. At zirconium concentrations of 0.01 to 1.0 M, the $\text{ZrOCl}_2 \cdot 8\text{H}_2\text{O}$ solid is completely dissociated into stable cations. The soluble compound $\text{ZrOCl}_2 \cdot 8\text{H}_2\text{O}$ is a tetramer of composition $[\text{Zr}(\text{OH})_2 \cdot 4\text{H}_2\text{O}]_4^{8+}$, that forms hydrous zirconia, $\text{ZrO}_x(\text{OH})_y \cdot n\text{H}_2\text{O}$.

In this experiment we prepared an aqueous solution of hydrous zirconia at a ZrOCl_2 concentration of 0.5 mol/L.

The hydrolysis and precipitation reaction is as follows:



The precipitation reaction in Equations (3) - (5) can be compiled as follows:



A hydrous zirconia sol was synthesized by boiling the aqueous solutions at 90°C for 2 h in a flask with a reflux condenser. An excess of HCl and NH_4OH was added to the ZrOCl_2 aqueous solution, in which H^+ and Cl^- ions are influencing the formation of secondary particles.^{3-6,15-20} The hydrous zirconia sol was then transported to the ED reactor (Fig. 3). The ED process was very effective for removal of Cl^- ions from the precipitates to make pure zirconia products. Fig. 4(a) shows an in situ observation image for a liquid

drop of slurry sample, which was picked up from the ZrOCl_2 solution during its hydrolysis at 90°C. A drop of fine hydrous-zirconia particles was put on a slide in an inverted optical microscope [OM]. During observation, the in situ morphology changed as the particles dried and these changes were saved as a dynamic image file. Fig. 4(b) shows one of the OM images of a slurry sample at the end of the ED process. The enlarged image in Fig. 4(b) shows nano-cluster aggregates composed of ~100 nm particles. The dimensions of the cluster aggregates was estimated to be from 5 to 20 μm. It is thought that particles as large as ~100 nm might be formed by coagulation of ~30 nm sols. In Fig. 4(a) and (b), we can observe several kinds of nano clusters and μm-sized aggregates. This means that various kinds of hydrous-zirconia complexes exist in chlorinated water. The zirconia polymeric sols are changed to gel state by removal of Cl^- by the ED process. The hydrous precipitates are formed during the transformation of polymeric sol-gel.

Figure 4(c) shows FE-SEM images of the morphology of the dry samples of hydrous zirconia particles obtained at the end of de-chlorination by the ED process. Note that this morphology shows a uniform distribution of nano-particles having diameters of 5 - 7 nm. The uniform nano-particles coagulate during drying. It is important to control particle coagulation in order to produce uniformly-distributed powder granules for sample shaping in the sintering process.

During the de-chlorination process the tetramer complex form, $[[\text{Zr}(\text{OH})_2 \cdot 4\text{H}_2\text{O}]_4]^{8+}$ may be changed to $[[\text{Zr}(\text{OH})_{2+x} \cdot (4-x)\text{H}_2\text{O}]_4]^{(8-x)+}$ according to the processes of de-protonation and de-chlorination.^{19,21} The particle size of $\text{Zr}(\text{OH})$ is controlled by $[\text{Zr}^{4+}]$ and temperature. With the removal of $[\text{Cl}^-]$ from $\text{Zr}[\text{OH}][\text{Cl}]$, complex polymer gel is formed from $\text{Zr}[\text{OH}]$ in aqueous solution. That is, a polymeric gel is formed from the mixed solution of hydrous zirconia, $\text{Zr}[\text{OH}]$ sol. During the extraction of $[\text{Cl}^-]$ supersaturated nucleation occurs, and crystal nuclei will form and grow to become nano-crystalline particles.²⁰⁻²³

Actually, the zirconia-complex solution got less viscous with the removal of $[\text{Cl}^-]$, and white crystallites were visible in the viscous $\text{Zr}[\text{OH}]$ solution. The viscous gel finally changed to white crystallites. In order to initiate the crystal-

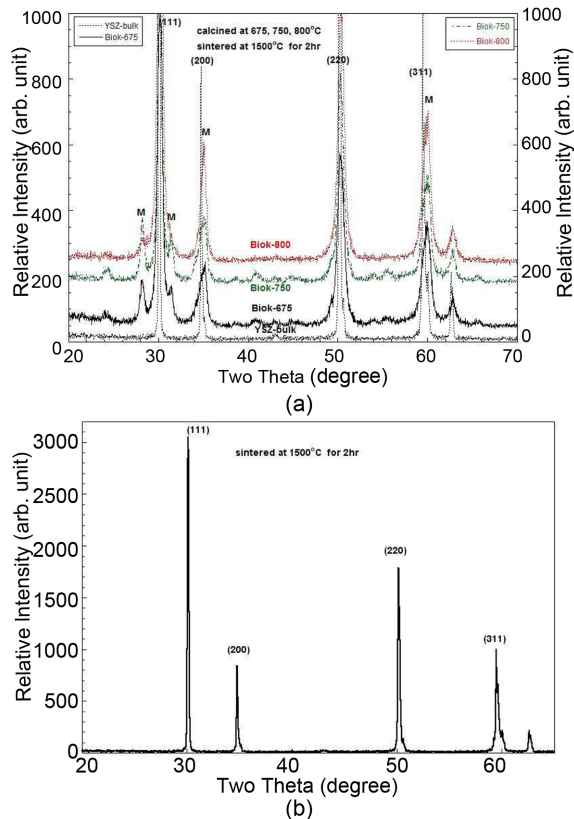


Fig. 5. (a) XRD analysis for the YSZ powders, which were fired at 675°C, 750°C, and 800°C and (b) XRD patterns for the sample body sintered at 1500°C.

lization process, the slurry solution in the ED reactor was slowly stirred. As crystallization proceeded the slurry-solution got less viscous and more easily stirred. Full de-chlorination took 10 h, as indicated by the appearance of the current value of 0.03 A. This means that the Cl^- ions attached to the zirconia complex were not as easy to dissociate as free Cl^- ions. It seems that the nano-cluster aggregates in Fig. 4(b) were organized by coagulation of nanoparticles, which were prepared from polymeric hydrous zirconia. The phase-change from polymeric zirconia sol-gel to nano-crystalline particles was greatly activated by the ED process, which was removing Cl^- ions from the complex compound.

For investigating the morphological kinetics of the hydrous zirconia complexes, the hydrous radius and zeta potential determined by laser scattering would be better, and the results will be discussed with the above-mentioned OM micrographs in another publication.

3.2. Yttrium stabilized zirconia powders and sintering

From Fig. 4(c), it can be seen that the particle size of zirconia powders is 5 to 7 nm. In this experiment the hydrous zirconia slurries were stirred in a beaker for an hour after termination of the de-chlorination process, and finally a solution of ethyl alcohol was added to uniformly disperse

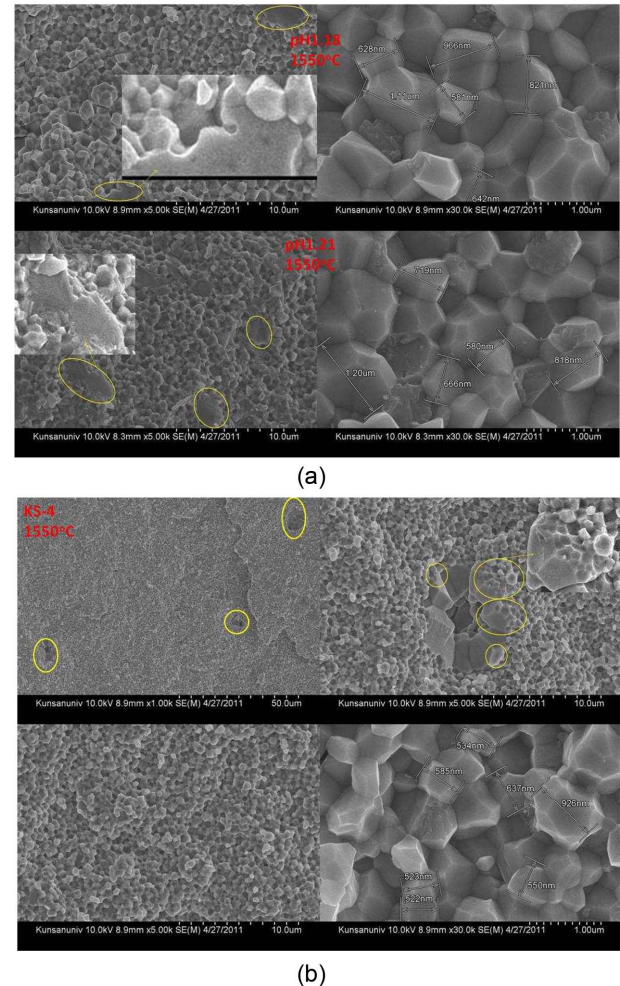


Fig. 6. SEM microstructure for the 3YSZ samples which were sintered at 1500°C for 2 h. (a) Sample bodies prepared at pH 1.18 and pH 1.21. The enlarged images in pH 1.18 and pH 1.21 show the grain growth. (b) Sintered body shows the exaggerated grain growth due to coagulation of nm-sized hydrous zirconia particles during drying. Circled and enlarged images show the abnormal grain growth. One μm sized grains are attached on the surface of bigger grains.

the slurry particles.²³⁾ The slurry solution was washed using a vacuum filter and the slurry paste so obtained was dried at 70°C in a drier for 10 h.

Yttrium-stabilized zirconia [YSZ] powders could be obtained by the calcination of $(\text{Zr},\text{Y})(\text{OH})_4$ precipitates prepared by the ED process. From the XRD analysis in Fig. 5(a) the zirconia powders calcined at 675 - 800°C showed a tetragonal phase with a minor amount of monoclinic phase.²¹⁻²³⁾ Tetragonal phase intensity gradually increased with the increase of firing temperature, and the XRD intensity of the monoclinic phase decreased. In Fig. 5(b), it can be seen that the body sintered at 1500°C showed critically-tetragonal peak patterns. The sintered body showed a highly dense microstructure with uniform grain.

The SEM images in Fig. 6 show the microstructure of

samples of YSZ-pH 1.18 and YSZ-pH 1.21 sintered at 1500°C for 2 h. The powder samples of YSZ-pH 1.18 and YSZ-pH 1.21 were prepared at pH 1.18 and pH 1.21, respectively. In Fig. 6(a), the YSZ-pH 1.21 sample shows locally exaggerated grain growth due to particle coagulation. The grain growth might be greatly affected by particle coagulation during drying. Additionally, there could be other influential factors such as the uniform-shaping density for the sample bodies. In Fig. 6(b), exaggerated grain growth is well observed. In the enlarged picture, several μm-sized grain surfaces are three-dimensionally connected with smaller grains. One μm sized grain was attached to the surface of several other μm-sized grains. The size distribution of one μm sized granule is between 500 nm and 900 nm. From these results, the appearance of abnormal grain might be due to particle coagulation. Controlling particle coagulation should yield highly dense bodies with uniform grain size, after sintering at 1500°C.

4. Conclusions

Hydrous zirconia particles were synthesized by hydrolysis of ZrOCl₂ solutions and the *in situ* morphology of the hydrous zirconia sol was observed under an optical microscope. The polymeric zirconia sol was de-chlorinated using the ED process and pure YSZ powders without Cl⁻ were obtained. FE-SEM images showing the microstructure of the pure YSZ particles showed the aggregation of nano particles. The sintered body prepared using the YSZ powders showed higher density and good uniformity in the grain microstructure.

REFERENCES

1. A. Clearfield, "Crystalline Hydrous Zirconia," *Inorg. Chem.*, **3** [1] 146-48 (1964).
2. A. Clearfield, "Structural Aspects of Zirconium Chemistry," *Rev. Pure Appl. Chem.*, **14** [1] 91-108 (1964).
3. K. Matsui and M. Ohgai, "Formation Mechanism of Hydrous-Zirconia Particles Produced by Hydrolysis of ZrOCl₂ Solutions," *J. Am. Ceram. Soc.*, **80** [8] 1949-56 (1997).
4. K. Matsui and M. Ohgai, "Formation Mechanism of Hydrous-zirconia Particles Produced by Hydrolysis of ZrOCl₂ Solutions: II," *J. Am. Ceram. Soc.*, **83** [6] 1386-92 (2000).
5. K. Matsui and M. Ohgai, "Formation Mechanism of Hydrous Zirconia Particles Produced by the Hydrolysis of ZrOCl₂ Solutions: III, Kinetics Study for the Nucleation and Crystal-growth Processes of Primary Particles," *J. Am. Ceram. Soc.*, **84** [10] 2303-12 (2001).
6. K. Matsui and M. Ohgai, "Formation Mechanism of Hydrous Zirconia Particles Produced by Hydrolysis of ZrOCl₂ Solutions: IV, Effects of ZrOCl₂ Concentration and Reaction Temperature," *J. Am. Ceram. Soc.*, **85** [3] 545-53 (2002).
7. R. Srinivasan and B. H. Davis, "Influence of Zirconium Salt Precursors on the Crystal Structures of Zirconia," *Catal. Lett.*, **14** [2] 165-70 (1992).
8. K. Matsui and M. Ohgai, "Phase Transformation of Hydrous-zirconia Fine Particles Containing Cerium Hydroxide," *J. Am. Ceram. Soc.*, **82** [11] 3017-23 (1999).
9. Hevesy G. v., Recherches sur le Propriétés du Hafnium; Det. Kg. Danske Videnska b. Selskab. VI, 7 143, 1925.
10. P. Schmid, "Über die Gewinnung von Zirkonoxyd und über die Konstitution Einiger Zirkonsalze," *Z. Anorg. Allgem. Chem.*, **167** 369-84 (1927).
11. H. J. Rapp and P. H. Pfromm, "Electrodialysis for Chloride Removal from the Chemical Recovery Cycle of a Kraft Pulp Mill," *J. Membr. Sci.*, **146** [2] 249-61 (1998).
12. V. Geraldes and M. D. Afonso, "Limiting Current Density in the Electrodialysis of Multi-ionic Solutions," *J. Membr. Sci.*, **360** [1] 499-508 (2010).
13. M. C. Chang, C. C. Ko, and W. H. Douglas, "Preparation of Hydroxyapatite-gelatin Nanocomposite," *Biomaterials*, **24** 2853-62 (2003).
14. M. C. Chang and R. DeLong, "Calcium Phosphate Formation in Gelatin Matrix Using Free Ion Precursors of Ca²⁺ and Phosphate Ions," *Dent. Mater.*, **25** [2] 261-68 (2009).
15. J. R. Fryer, J. L. Hutchison, and R. Paterson, "An Electron Microscopic Study of the Hydrolysis Products of Zirconyl Chloride," *J. Colloid Interface Sci.*, **34** [2] 238-48 (1970).
16. A. Nagai, M. Hirano, Y. Murase, Y. Kobasashi, and E. Kato, "Formation Mechanism of Fine Anisotropically-Shaped m-ZrO₂ Crystals in Thermal Hydrolysis of Sulfate Solution," *J. Ceram. Soc. Jpn.*, **103** [6] 610 (1995).
17. C. F. Baes, Jr. and R. E. Mesmer, *The Hydrolysis of Cations*; p. 427, Wiley, New York, 1976.
18. W. B. Blumenthal, "The Chemical Behavior of Zirconium, Chapters 3, 4, & 6", D. van Nostrand Co., New York, 1958.
19. A. Clearfield and P. A. Vaughan, "The Crystal Structure of Zirconyl Chloride Octahydrate and Zirconyl Bromide Octahydrate," *Acta. Cryst.*, **9** [7] 555-58 (1956).
20. J. S. Johnson and K. A. Kraus, "Hydrolytic Behavior of Metal Ions. VI. Ultracentrifugation of Zirconium (IV) and Hafnium (IV); Effect of Acidity on the Degree of Polymerization," *J. Am. Chem. Soc.*, **78** [16] 3937-43 (1956).
21. G. M. Muha and P. A. Vaughan, "Structure of the Complex Ion in Aqueous Solutions of Zirconyl and Hafnyl Oxyhalides," *J. Chem. Phys.*, **33** [1] 194-99 (1960).
22. A. Bleir and M. Cannon, "Nucleation and Growth of Uniform m-ZrO₂," *Mater. Res. Soc. Symp. Proc.*, **73** 71-78 (1986).
23. K. Matsui, H. Suzuki, M. Ohgai, and A. Arashi, "Raman Spectroscopic Studies on the Formation Mechanism of Hydrous-zirconia Fine Particles," *J. Am. Ceram. Soc.*, **78** [1] 146-52 (1995).